Schizophrenia Bulletin vol. 40 no. 3 pp. 675–684, 2014
doi:10.1093/schbul/sbt050
Advance Access publication April 24, 2013

Diagnostic Discontinuity in Psychosis: A Combined Study of Cortical Gyrification and Functional Connectivity

Lena Palaniyappan* and Peter F. Liddle

Division of Psychiatry, Institute of Mental Health, University of Nottingham, Nottingham, UK

*To whom correspondence should be addressed; Room-09, C Floor, Institute of Mental Health Building, Triumph Road, Nottingham, NG7 2TU, England, UK; tel: +44 (115) 823 0407, fax: 44 (115) 823 0433, e-mail: Lena.Palaniyappan@nottingham.ac.uk

The point of rarity in brain structure and function that separates the 2 major psychotic disorders—schizophrenia and bipolar disorder—is presently unknown. The aim of this study is to combine surface anatomical and functional imaging modalities to quantify the integrity of cortical connectivity in pursuit of the neural basis of the Kraepelinian "line of divide." We tested the hypothesis that multimodal brain regions show overlapping abnormalities in both disorders, while schizophrenia-specific defects are likely to be localized to sensory processing regions. Cortical folding patterns (gyrification) and functional connectivity hub architecture (degree centrality) were studied in a sample of 39 subjects with established schizophrenia, 20 subjects with psychotic bipolar disorder, and 34 healthy controls. We observed a significant difference between the 2 groups in both gyrification and functional connectivity of the visual processing regions. Further, the aberrant functional connectivity of the visual processing regions predicted persistent symptom burden better than the diagnostic information. Using a spatial similarity analysis, we observed that the degree of overlap between the 2 disorders was small (25%) for changes in cortical gyrification and modest (51%) for changes in functional connectivity measured during a cognitive task (*n*-back). In conclusion, our results suggest that prominent unimodal sensory processing deficits are more likely to be present in schizophrenia than in bipolar disorder. Further, connectivity-based neuroimaging measures appear to be better indicators of diagnostic discontinuity than the symptom-based clinical information.

Key words: Kraepelinian/bipolar disorder/visual processing/insula/gyrification/schizophrenia

Introduction

Significant nosological uncertainty over Kraepelin's description of 2 major psychotic disorders persists to date. While several observations suggest the existence of overlapping pathophysiological processes in schizophrenia and bipolar disorder,[1] the point of rarity in brain structure and function at which the 2 disorders differ is elusive.

Structural imaging studies have mostly used voxel-based morphometric approach to differentiate the 2 disorders. So far, direct comparisons have not established any regional brain changes that separate these 2 illnesses. It is possible that subtle changes exist in the surface anatomy that is not captured by studying volumetric changes in the gray matter.[2] Some support for this notion comes from Rimol et al.[3] who observe that while volume changes occur in both groups, deformation of the cortical surface appears more specific to schizophrenia. Cortical gyrification (or folding) is a promising surface anatomical marker to study schizophrenia and bipolar disorder.[4] Cortical folding patterns are established during early phases of development and are likely to be affected by a higher burden of aberrant neurodevelopment reported in schizophrenia.[5] In addition, because folding patterns are tightly linked to underlying neural connectivity,[4] gyrification appears to be a compelling candidate to investigate the Kraepelinian dichotomy.

There is an increasing realization that the functional integration, rather than regional specialization in the brain, is likely to be abnormal in psychosis, with several studies in schizophrenia suggesting an inefficient recruitment of distributed brain regions during task performance.[6] To date, fMRI studies contrasting bipolar disorder and schizophrenia have mostly used task activation approaches and observed similar regional brain dysfunction in both disorders.[1] This approach does not directly address the possible differences that may exist in the efficiency of cerebral recruitment in the 2 groups and fails to capture the system-level disintegration in the neural networks. In recent times, several approaches have been proposed to measure the integrative functions of brain regions using fMRI. A promising method is

studying the number of instantaneous functional connections (or correlations) between a region and the rest of the brain, also called degree centrality (DC).[7] This approach has established the notion of cortical hubs, specialized brain regions that show high DC and thus influence a number of other brain regions. The core architecture formed by cortical hubs is consistent and stable in healthy human brain but highly vulnerable to pathological processes.[7,8] Both structural and functional studies indicate the loss of prominence of multimodal cortical hubs and the emergence of peripheral hubs in unimodal cortex in schizophrenia.[9,10] Whether such a shift in the cortical topology is specific to schizophrenia is yet to be investigated.

Behavioral[11] and electrophysiological studies[12] comparing patients with bipolar disorder schizophrenia suggest that early sensory processing deficits may be specific to schizophrenia, with fMRI studies finding converging group differences localized to unimodal regions such as the extrastriate visual association cortex.[13,14] On the other hand, paralimbic brain regions constituting large-scale brain networks such as the insula and anterior cingulate cortex show prominent but shared structural alterations in the 2 disorders.[15] In the light of these observations, we hypothesized that across the 2 psychotic disorders, overlapping abnormalities in the structure and function will involve the multimodal brain regions and the limbic/paralimbic cortex, while schizophrenia specific defects will be restricted to unimodal sensory processing areas.

We recruited a sample of patients with either bipolar disorder with psychotic symptoms (BPP) or schizophrenia (SCZP) and healthy controls and studied the cortical gyrification from structural magnetic resonance imaging (MRI) and the DC from functional MRI using an executive/working memory task (*n*-back). In addition to examining the integrity of the core cortical hub architecture, we also examined for the emergence of peripheral hubs in patients. The 3 groups were compared with each other; in addition, we also performed conjunction analyses to identify the degree of overlap (or similarity) in the abnormalities common to both disorders. In line with Kraepelin's original claim of interepisode recovery/symptom burden differentiating the 2 disorders,[16] we expected the neurobiological features that differentiate the 2 psychotic disorders to be associated with the persisting severity of clinical symptom burden in the clinically stable phase.

Methods

Participants

The sample consisted of 39 patients satisfying DSM-IV criteria for schizophrenia, 20 patients with bipolar disorder with psychotic features, and 34 healthy controls. Patients were recruited from the community-based mental health teams (including Early Intervention in Psychosis teams) in Nottinghamshire and Leicestershire, United Kingdom. The diagnosis was made in a clinical consensus meeting in accordance with the procedure of Leckman et al.,[17] using all available information including a review of case files and a standardized clinical interview (Symptoms and Signs in Psychotic Illness [SSPI]).[18] All patients were in a stable phase of illness (defined as a change of no more than 10 points in their Global Assessment of Function [DSM-IV] score, assessed 6 weeks prior and immediately prior to study participation). No patient had a change in antipsychotic-, antidepressant-, or mood-stabilizing medications in the 6 weeks prior to the study. Subjects with age <18 or >50, with neurological disorders, current substance dependence, or intelligence quotient < 70 using Quick Test[19] were excluded. Fifty-four out of 59 patients were receiving psychotropic medications. The median Defined Daily Dose (DDD)[20] was calculated separately for antipsychotics, mood stabilizers (including lithium), and antidepressants (see online supplementary material SM1). Patients were interviewed on the same day as the scan and symptom scores assigned according to the SSPI.

Healthy controls were recruited from the local community via advertisements, and 34 subjects free of any psychiatric or neurological disorder group-matched for age and parental socioeconomic status (measured using National Statistics–Socio Economic Classification)[21] were included to the patient group. Controls had similar exclusion criteria to patients; in addition, subjects with personal or family history of psychotic illness were excluded. A clinical interview by a research psychiatrist was employed to ensure that the controls were free from current axis 1 disorder and history of either psychotic illness or neurological disorder. The study was given ethical approval by the National Research Ethics Committee, Derbyshire, United Kingdom. All volunteers gave written informed consent. See online supplementary material SM2 for details on the excluded subjects and other sample characteristics.

Data Acquisition

Blood oxygenation level-dependent (BOLD) fMRI data sets were acquired on a 3-T Philips Achieva MRI scanner (Philips, the Netherlands). To enhance sensitivity, dual-echo gradient-echo echo-planar images (GE-EPI) were acquired,[22] using an 8-channel SENSE head coil with SENSE factor 2 in anterior-posterior direction, TE1/TE2 25/53 ms, flip angle 85°, 255 mm × 255 mm field of view, with an in-plane resolution of 3 mm × 3 mm and a slice thickness of 4 mm, and TR of 2500 ms. At each dynamic time point, a volume data set was acquired consisting of 40 contiguous axial slices acquired in descending order. A total of 410 dynamic time points were acquired during an entire *n*-back session, with 2 sessions in total per subject. A magnetization-prepared rapid acquisition gradient echo image with 1 mm isotropic resolution, 256 × 256 × 160 matrix, Repetition Time (TR)/Echo Time (TE)

8.1/3.7 ms, shot interval 3 s, flip angle 8°, SENSE factor 2 was also acquired for each participant for reconstructing the anatomical surface.

fMRI Task

We used a visual *n*-back task with a button press response in 2 sessions of fMRI recording. Seven task blocks each of 110 s duration were presented in each session. Each task block consisted of 0-back, 1-back, and 2-back conditions of 30 s duration each presented in a random sequence, with 10 s interval between the conditions. On-screen instructions preceded every condition indicating the type of response required (0-, 1-, or 2-back). Each condition included 4 target and 11 nontarget stimuli with a 2 s interstimulus interval. To ensure adequate task comprehension and performance, all participants performed a practice version of the task outside the scanner prior to scanning. All scanned participants successfully identified in excess of 80% of targets in the practice task.

fMRI Preprocessing

fMRI data were preprocessed using SPM8 and the DPARSFA/REST software[23] (see online supplementary material SM2 for details). Preprocessed data were analyzed by deriving degree of centrality (DC) measure for every gray matter voxel using the cortical hub analysis procedure described by Buckner et al.,[7] and implemented in the REST software.[23] For each voxel, we extracted the BOLD time course and correlated with every other voxel in the brain. For each voxel *j*, the number of strong voxel-to-voxel correlations (defined as correlation coefficient $r > 0.25$) was computed to determine the DC of *j*. The threshold of 0.25 was chosen to minimize the risk of inclusion of voxels whose correlation with the index voxel could be accounted for by noise in the centrality estimate for the index voxel. For each subject, a map with DC values for every gray matter voxel was obtained. These maps were then *z*-transformed to enable group comparisons. The computation of normalized DC maps was done separately for both resting state acquisition and the *n*-back acquisition.

Surface Extraction

Cortical surfaces were reconstructed using FreeSurfer version 5.1.0. The preprocessing was performed using standard procedures as described by Dale et al.[24] To measure cortical folding patterns for each of the several thousands of vertices across the entire cortical surface, we used the method advocated by Schaer et al.[25] This method provides Local Gyrification Indices (LGIs), numerical values assigned in a continuous fashion to each vertex of the reconstructed cortical sheet. The LGI of a vertex corresponds to the ratio of the surface area of the folded pial contour ("buried" surface) to the outer contour of the cortex ("visible" surface) included within a sphere of 25 mm radius drawn around each vertex. Thus the LGI value at each vertex reflects the amount of cortex buried in its immediate locality.

Statistical Analysis

Core Hub Centrality. To determine the core cortical hub architecture, we identified the significant clusters with high DC across the entire sample using 1 sample *t* test (familywise error [FWE]-corrected error rate of 5%, cluster extent threshold = 30 voxels). We computed a single mean value of the normalized DC measure in each voxel included in the core hubs for each subject, which represented the mean DC of the core (DCC). We used an ANCOVA to compare the DCC among the 3 groups, after taking into account the effect of age and gender. We also tested the effect of including the overall *n*-back accuracy scores as covariates because this was significantly different among the groups.

Spatial Distribution of Group Differences. To examine the differences between the 2 disorders in DC on a voxelwise basis across the entire brain, we derived direct between-group comparisons (SCZP vs BPP contrast) with an FWE-corrected type-1 error rate of 5% at a voxelwise threshold of $P = .001$. We also compared each patient group with the control group, at the same statistical threshold. All group comparisons included age, gender, and *n*-back accuracy scores as covariates.

Gyrification Analysis

The vertexwise LGI measurement for each subject was mapped on a common spherical coordinate system (*fsaverage*) to enable group comparisons. A general linear model controlling for the effect of age and gender was used to compute differences in gyrification between the groups at each vertex of the right and left hemispheric surfaces. Query Design Estimate Contrast tool in the Freesurfer program was used to generate the contrasts. To correct for multiple testing, we used Monte-Carlo simulations ($n = 10\,000$) and identified clusters that survived a type-1 error rate of 5% at a cluster inclusion threshold of $P = .05$. In a different sample of subjects, we have previously shown that both increased and decreased gyrification in schizophrenia are observable at this threshold.[31]

Degree of Overlap Between the 2 Disorders

To compute the topographical overlap in the abnormalities seen in BPP and SCZP, we derived an intersection (overlap) mask and a combination (union) mask for the contrasts controls vs SCZP and controls vs BPP. We then calculated the Dice Coefficient of Similarity (DCS)[8,26] between the 2 groups for the 2 imaging modalities (DC and gyrification maps). Conjunction measures such as DCS provide more reliable results when every signal of interest is included in the individual contrasts.[27] To enable

this, we used an uncorrected threshold of $P = .05$ when extracting the intersection and the combination masks. A DCS value of 100% means that both the disorders have perfect spatial agreement in the distribution of abnormalities across the brain.

Relationship With Symptom Burden

We performed multiple regression analysis with the DC and gyrification measures extracted from the clusters showing significant differences in the SCZP vs BPP contrast as independent variables, in addition to the diagnostic status to predict the total SSPI score (dependent variable). We expected this analysis to reveal the neural correlates of total symptom burden in the 2 disorders, over and above the utility of the diagnostic categories. We also repeated this analysis with 3 syndrome scores (Reality Distortion, Psychomotor Poverty, and Disorganization) as independent variables.

Results

The core hub regions showing significant DC in the entire sample is shown in table 1 (online supplementary figure SF1). Comparison of the mean DCC across the 3 groups revealed no significant differences ($F[2,88] = 1.25$, $P = .29$; mean [SD] of DCC in controls = 0.54 (0.23), SCZP = 0.46 (0.32), and BPP = 0.47 (0.17)). Age ($F[1,88] = 16.4$, $P < .001$), but not gender ($F[1,88] = 1.35$, $P = .25$), had a significant effect on DCC. The inclusion of *n*-back accuracy or the exclusion of age and gender as covariates did not affect the results.

Voxelwise comparisons revealed significant differences among the groups (table 2) in the DC of several brain regions. In particular, both groups of patients showed higher DC in bilateral hippocampus/parahippocampal regions extending to the thalamus (figure 1). In addition, SCZP showed significant increase in DC in left fusiform/lingual and inferior occipital gyrus. Compared with BPP, SCZP showed higher centrality in left calcarine/lingual gyrus and anterior cerebellum but reduced DC in right supramarginal gyrus.

Significant group differences were also noted in gyrification, with more prominent reduction in the SCZP. Right lingual, left posterior cingulate, and bilateral orbital frontoinsular regions show reduced gyrification in SCZP compared with BPP (see table 3 and online supplementary material SF2).

We repeated the DC analysis using resting fMRI scans obtained from the same sample. These results are presented in the online supplementary material (SM3). Regions showing combined gyrification and DC differences in SCZP vs BPP contrasts are displayed in figure 2. The DCS test revealed 25% overlap in the topography of gyrification abnormalities and 51% overlap in the topography of DC abnormalities between BPP and SCZP, compared with controls (see online supplementary material SM4).

Regression analysis revealed that the DC in left calcarine/lingual cortex ($\beta = 0.33$, $P = .02$), rather than the diagnostic classification ($\beta = 0.21$, $P = .23$), significantly predicted the total symptom burden (especially the Reality Distortion [$\beta = 0.37$, $P = .01$]) during clinical stability. None of the other predictors were significant in this model (all $P > .2$). For Psychomotor Poverty, DC of right supramarginal cluster ($\beta = -0.33$, $P = .03$) was a significant predictor with diagnosis having a trend level significance ($\beta = 0.3$, $P = .08$; see online supplementary material SM4 for more details).

Table 1. Coordinates of Maximum Clusters Derived From Whole-Brain Analysis of Degree Centrality Representing Significant Cortical Hubs in the Entire Sample, Including Patients and Controls (FWE-Corrected $P < .05$, $k = 30$)

Brain Region	Peak MNI Coordinates (x, y, z) in mm	Peak *T* Intensity	Cluster Extent (Number of Voxels)
Left inferior/superior parietal lobule and superior temporal gyrus	−42, −42, 42	13.66	1433
Right inferior/superior parietal lobule and superior temporal gyrus	48, −42, 45	13.21	1381
Posterior cingulate/precuneus	−6, −48, 24	12.76	488
Medial superior frontal gyrus	3, 15, 45	12.65	1332
Right middle/inferior frontal gyrus (DLPFC)	42, 39, 24	11.72	691
Left cerebellar crus	−9, −75, −27	10.97	150
Left middle/inferior frontal gyrus (DLPFC)	−48, 9, 27	10.40	270
Right cerebellar crus	30, −63, −33	9.14	67
Left middle temporal gyrus	−57, −12, −24	8.14	51
Right inferior temporal gyrus	57, −9, −30	7.84	45
Right inferior temporal gyrus	51, −51, −15	7.76	67
Left precentral gyrus	−30, 0, 57	7.21	49
Left superior temporal gyrus	−51, 0, 0	6.70	52
Right lingual/fusiform gyrus	21, −72, −9	6.47	77

Note: DLPFC, Dorsolateral Prefrontal Cortex; FWE, cluster level familywise correction for multiple comparisons.

Table 2. Degree Centrality Differences Between Patients and Controls During *n*-Back Task (Uncorrected $P < .001$, $k = 30$)

Comparison	Brain Region	Peak MNI Coordinates (x, y, z) in mm	Peak *T* Intensity	Cluster Extent (Number of Voxels)
Controls > Schizophrenia	Right superior temporal gyrus[a]	33, 6, −24	5.39	48
	Right insula[a]	45, −15, 3	4.95	137
	Left superior frontal gyrus	−3, 36, 60	4.54	35
	Left inferior frontal gyrus[a]	−39, 24, 12	4.37	64
	Left inferior parietal lobule	−42, −54, 42	4.24	37
Controls > Bipolar	Right insula[a]	45, −12, 3	4.51	102
Schizophrenia > Controls	Left fusiform, lingual and inferior occipital gyrus[a]	−21, −81, −9	6.29	434
	Bilateral hippocampus, parahippocampal gyrus and thalamus[a]	−36, −33, −12	5.72	438
	Right fusiform, lingual and inferior temporal gyrus	36, −63, −12	4.58	154
Bipolar > Controls	Right hippocampus and parahippocampal gyrus[a]	24, −24, −9	5.59	164
	Left hippocampus, parahippocampal gyrus and[a] thalamus	−30, −42, −3	5.31	363
	Left caudate	−9, 6, −12	4.47	49
	Right inferior temporal	51, −48, −27	4.37	51
Bipolar > Schizophrenia	Right supramarginal gyrus[a]	57, −39, 39	4.24	96
Schizophrenia > Bipolar	Cerebellum Anterior Lobe[a]	36, −48, −30	4.80	83
	Left calcarine sulcus and lingual gyrus[a]	−6, −84, 0	3.85	37

[a]Regions that survive cluster level familywise correction at $P < .05$ for multiple comparisons.

Discussion

To our knowledge, this is the first study to use combined surface anatomical and functional connectivity approach to study the neural basis of the diagnostic discontinuity in psychosis. We have shown that while a degree of overlap exists between the 2 disorders in the functional connectivity and cortical gyrification, significant differences between the disorders are notable especially in the visual processing regions. While the core hub of functional connectivity seems to be preserved in both patient groups, the emergence of a higher degree of connectivity in the hippocampus/parahippocampus and thalamic regions and a reduction in the connectivity of the right insula were observed in both patient groups. An overlapping reduction in gyrification was also noted in the lateral prefrontal cortex in both patient groups. In contrast, the 2 groups showed significant differences in cortical gyrification and functional connectivity involving calcarine, lingual, and fusiform regions and, to some extent, the left insula and middle temporal gyrus.

A reduction in the centrality of right insula in both groups is consistent with a large body of evidence implicating this region in the emergence of psychotic symptoms.[28] In both SCZP and BPP, peripheral hubs emerged in the parahippocampal complex extending to the thalamus. This is consistent with Meyer-Lindenberg et al.'s[29] observation of inappropriate recruitment and connectivity of the parahippocampal regions during working memory performance in schizophrenia. It is important to note that the regional distribution of the connectivity differences is likely to differ according to the cognitive paradigm used. For example, an overactivation of medial temporal structures in BPP compared with those in SCZP has been noted when performing emotion/reward or memory based tasks but not in tasks involving language or executive functions.[1]

Interestingly, in contrast to the BPP who had an increase in the DC of lateral parietal cortex (supramarginal gyrus), part of the core connectivity hub, the SCZP displayed an increase in DC of the anterior cerebellum and extrastriate visual cortex during both *n*-back and resting state, suggesting a conjoint dysfunction of these 2 regions. Focused examination of cerebellar connectivity during rest suggests that amidst an overall reduction in the corticocerebellar connectivity, the connectivity between extrastriate visual cortex and cerebellum appears to be increased in SCZP.[30]

In line with our previous study in a different set of subjects with schizophrenia,[31,32] we observed a predominant reduction in gyrification involving lateral prefrontal region, insula, and superior temporal regions in SCZP. To our knowledge, this is the first study reporting vertexwise whole-brain gyrification defects in BPP. BPP had reduced gyrification predominantly involving lateral prefrontal and superior parietal regions compared with controls but showed increased gyrification in posterior cingulate and lingual gyrus compared with SCZP. The 2 groups showed relatively less spatial overlap in the extent of gyrification abnormalities (25%) compared with the functional connectivity measures. A recent postmortem

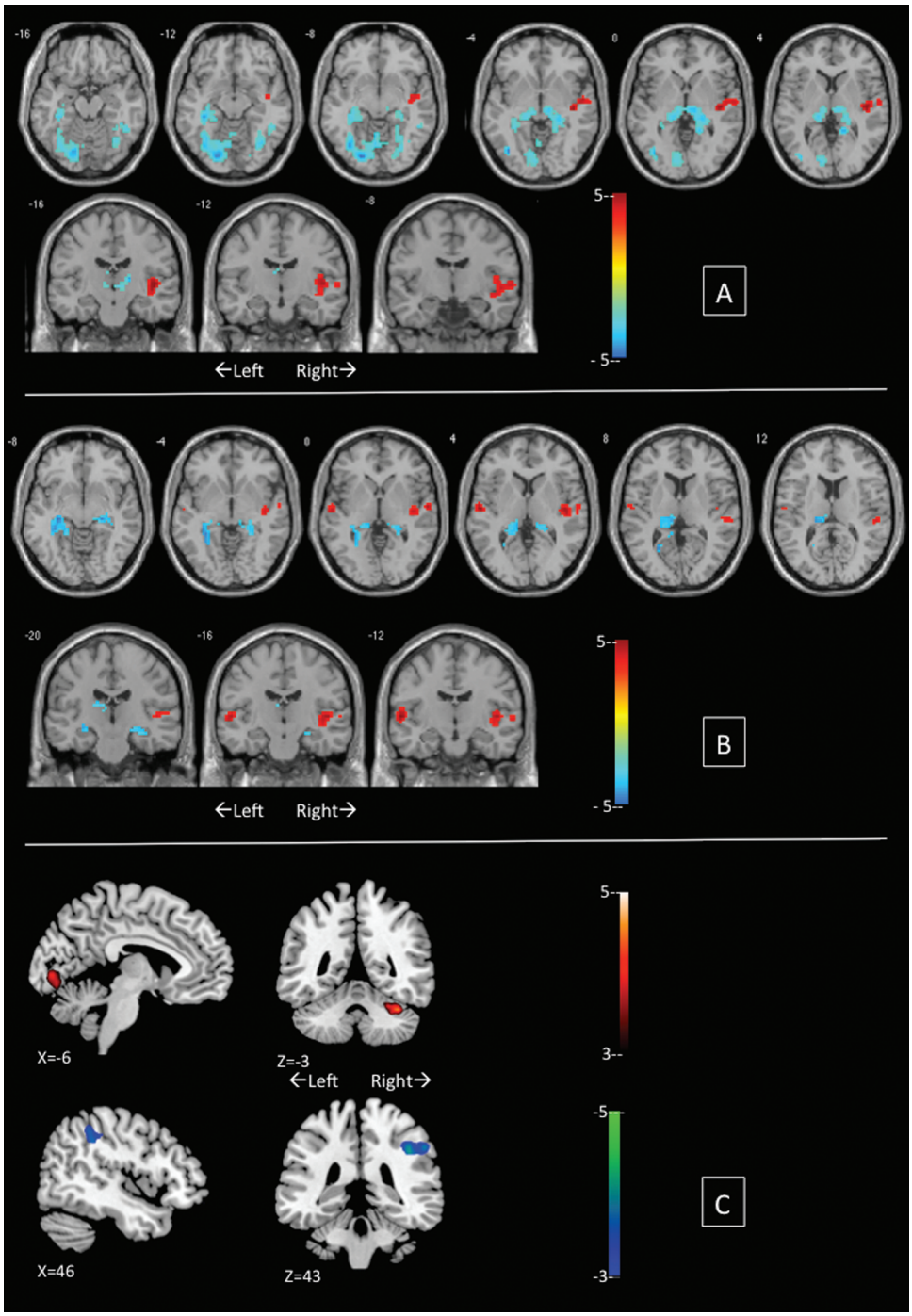

Fig. 1. Group differences in degree centrality from *n*-back fMRI in patients with schizophrenia compared with bipolar disorder. Illustrations drawn on a single subject structural image with slices selected for the best display of regions showing differences in the two sample *t* test. Top panel (A) displays schizophrenia vs controls contrast; middle panel (B) displays bipolar disorder vs controls contrast. In A and B, warm colors refer to higher degree centrality in controls. Bottom panel (C) shows schizophrenia > bipolar disorder contrast in the upper row and bipolar disorder > schizophrenia contrast in the lower row. Color bars show scales of *T* values. Panels A and B were created using xjview (www.alivelearn.net/xjview8). Panel C was created using MRICron (www.nitrc.org/projects/mricron). A color version of this figure is available online.

study suggests that abnormal gyrification in cerebellar vermis is a feature of schizophrenia.[33] Because the surface based morphometric approaches do not reconstruct the cerebellum, our gyrification analysis was restricted to the cerebral surface only.

In general, the spatial extent of both DC and gyrification abnormalities was numerically larger in SCZP than in BPP (online supplementry table 1 in SM4). Interestingly, the similarity coefficient was higher in the *n*-back than in the resting fMRI or gyrification analysis. This finding

Table 3. Gyrification Differences Between Patients and Controls (Cluster Inclusion Threshold $P = .05$)

Comparison	Brain Region	Peak MNI Coordinates (x, y, z) in mm	Clusterwise Probability	Cluster Extent in mm^2
Controls > Schizophrenia	Right caudal middle frontal[a]	36, 22, 44	.0001	3238
	Right inferior parietal/ superior temporal[a]	60, −55, 13	.0002	1430
	Right lingual	22, −69, −1	.012	916
	Left Insula[a]	−35, 5, −18	.001	1207
	Left precuneus/posterior cingulate[a]	−6, −45, 56	.0001	5847
	Left superior frontal[a]	−17, 46, 37	.0001	2680
	Left middle temporal[a]	−63, −50, 6	.0001	3360
	Left supramarginal[a]	−62, −23, 30	.0001	2446
Controls > Bipolar	Right caudal middle frontal[a]	36, 23, 42	.0001	3312
	Right rostral middle frontal	35, 39, 25	.0029	966
	Right superior parietal[a]	31, −38, 66	.0002	1231
	Right postcentral	56, −13, 38	.0457	633
	Right lateral occipital	53, −72, 14	.0335	671
	Left caudal middle frontal	−31, 28, 36	.0031	1093
	Left superior parietal/precuenus	−26, −45, 68	.046	722
Schizophrenia > Controls	None	—	—	—
Bipolar > Controls	Left fusiform gyrus[a]	−31, −69, −1	.0001	3022
	Left medial orbitofrontal	−5, 28, −32	.0333	559
Bipolar > Schizophrenia	Right lingual gyrus[a]	21, −69, −2	.0001	5533
	Right lateral orbitofrontal	22, 27, −27	.007	1005
	Left posterior cingulate[a]	−5, −8, 37	.0001	8573
	Left middle temporal	−64, −28, −11	.046	723
	Left insula/lateral orbitofrontal	−29, 20, −23	.007	981
Schizophrenia > Bipolar	None	—	—	—

[a]Clusters that survived correction for multiple comparisons using Monte-Carlo simulations ($n = 10\,000$ iterations; clusterwise probability $P = .001$).

highlights the importance of using multiple neuroimaging tools to investigate the current issue of diagnostic discontinuity. Further it suggests that when external constraints such as task demands are present, "schizophrenia-like" functional abnormalities are likely to appear in BPP.

Abnormal visual information processing appears to be specific to SCZP and their relatives compared with BPP and their relatives.[34] This corroborates our current findings that imply diagnostic specificity involving visual processing regions. It is worth noting that the extrastriate visual cortex, where we find combined gyrification and functional connectivity defects in schizophrenia, shows a predilection for developmental disturbances that affect cortical maturation.[35] Ongur et al.[14] found significantly reduced coherence between extrastriate visual cortex and other brain regions during rest in schizophrenia compared with bipolar disorder. Sui et al.,[36] using independent component connectivity analysis during auditory oddball task performance, observed a predominantly visual cortex component to discriminate SCZP from BPP. SCZP fail to recruit the extrastriate cortex during semantic decision and verbal fluency[13] but show greater engagement during facial affect processing compared with BPP.[37] Inefficient functional connections in these regions could result in inflated centrality but reduced task-related efficiency.[13] Further the observation that DC of left calcarine/lingual cortex is a better predictor of severity of symptoms (especially delusions and hallucinations) that persist in clinically stable psychotic patients, than in the categorical diagnostic grouping, suggests that the neural basis of the diagnostic separation along the continuum of the 2 major psychotic disorders is tightly linked to the integrity of extrastriate visual cortex. Independent of the clinical diagnostic boundaries, increased calcarine/lingual gyrus DC predicts higher burden of Reality Distortion, while reduced supramarginal DC predicts higher burden of Psychomotor Poverty in a clinically stable state. This suggests that patients with BPP and residual "interepisode" symptoms share a tendency to neuroanatomical abnormalities typical of schizophrenia.

A specific strength of this study is the recruitment of bipolar disorder cases who also experience psychotic symptoms during the course of their illness (BPP), in contrast to previous studies that recruited bipolar disorder irrespective of the presence of psychotic symptoms.[36,38] Further, we employed a multimodal approach studying structural and functional anatomy during rest and a cognitive task. Nevertheless, several limitations must be considered when interpreting these results. First, the sample size of BPP was small compared with that of SCZP and controls, but this is unlikely to have influenced the current results (see online supplementary material SM4). The overall proportion of female subjects was low though

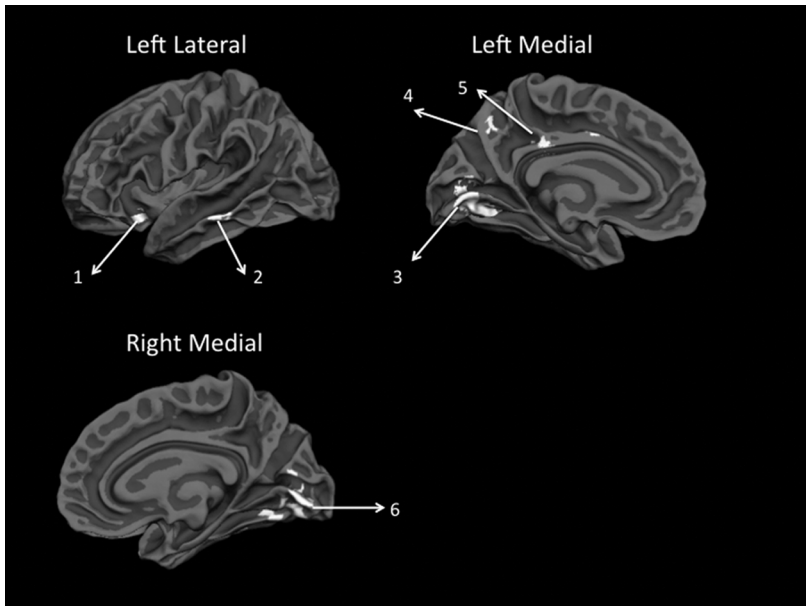

Fig. 2. Overlap between gyrification and degree centrality changes in the schizophrenia vs bipolar disorder contrasts. Both contrasts were thresholded at uncorrected $P < .05$ to increase the sensitivity of the conjunction analysis and displayed on white matter surface of reconstructed template cortical surface (*fsaverage*) using FreeSurfer. (1) Left anterior insula, (2) left middle temporal gyrus, (3) left lingual gyrus/calcarine fissure, (4) left precuneus, (5) left posterior cingulate, and (6) right lingual gyrus/calcarine fissure.

the groups were well matched for gender distribution. Most patients were taking antipsychotic medications, with several patients in the BPP also being exposed to mood stabilizers. To our knowledge, there is no evidence that these medications have differential effect on cortical gyrification or centrality measures though volumetric measures appear to be affected by both antipsychotics and lithium.[39] In our sample, we did not find significant associations between antipsychotic DDD (SCZP/BPP) or mood stabilizer DDD (BPP only) and core hub centrality or cortical gyrification (online supplementary material SM4). Existing evidence predicts that at least in the short-term, antipsychotics could reduce overall functional connectivity[40]; our observation that SCZP show higher connectivity in visual processing regions compared with BPP is in the opposite direction, suggesting that medications alone cannot explain all of the present findings. Nevertheless, we cannot completely exclude the effect of prescribed medications on the current observations.

Our study provides critical evidence delineating neurobiological underpinnings of the diagnostic boundaries of psychosis. Crucially, the observed neural correlates predict symptom burden during clinically stable state, highlighting the ability of connectivity based neuroimaging measures to inform nosological classification. Together with the emerging neuroimaging literature on high-risk states,[41,42] our observations open the question as to whether treatment selection during early psychosis could be better informed by utilizing neuroimaging markers that differentiate the 2 disorders, alongside the existing symptom-based decision-making.

Funding

Medical Research Council (G0601442); Wellcome Trust (Research Training Fellowship to LP).

Supplementary Material

Supplementary material is available at http://schizophreniabulletin.oxfordjournals.org.

Acknowledgments

We are grateful to all volunteers who participated in this study. Our sincere thanks to Vijender Balain, Marije Jansen, Thomas White, Molly Simmonite, Bert Park, and Elizabeth Liddle for their assistance. We are thankful to Robert Sommer Research Society for supporting the presentation of an abstract of this work at Giessen, Germany (March 2013). Conflicts of interest: L.P. has received a Young Investigator Travel Fellowship funded by Eli Lilly. In the past 5 years, P.F. Liddle has received honoraria for academic presentations from Janssen-Cilag and Bristol Myers Squibb, and has taken part in advisory panels for Bristol Myers Squibb.

References

1. Whalley HC, Papmeyer M, Sprooten E, Lawrie SM, Sussmann JE, McIntosh AM. Review of functional magnetic resonance imaging studies comparing bipolar disorder and schizophrenia. *Bipolar Disord*. 2012;14:411–431.

2. Palaniyappan L, Liddle PF. Differential effects of surface area, gyrification and cortical thickness on voxel based morphometric deficits in schizophrenia. *Neuroimage*. 2012;60:693–699.
3. Rimol LM, Nesvåg R, Hagler DJ Jr, et al. Cortical volume, surface area, and thickness in schizophrenia and bipolar disorder. *Biol Psychiatry*. 2012;71:552–560.
4. White T, Hilgetag CC. Gyrification and neural connectivity in schizophrenia. *Dev Psychopathol*. 2011;23:339–352.
5. Demjaha A, MacCabe JH, Murray RM. How genes and environmental factors determine the different neurodevelopmental trajectories of schizophrenia and bipolar disorder. *Schizophr Bull*. 2011. http://schizophreniabulletin.oxfordjournals.org/content/early/2011/08/19/schbul.sbr100.abstract. Accessed February 15, 2012.
6. Pettersson-Yeo W, Allen P, Benetti S, McGuire P, Mechelli A. Dysconnectivity in schizophrenia: where are we now? *Neurosci Biobehav Rev*. In Press, Corrected Proof. http://www.sciencedirect.com/science/article/B6T0J-51JXFM1-1/2/32237c0812eb8b9936761e0ec8970330. Accessed March 2, 2011.
7. Buckner RL, Sepulcre J, Talukdar T, et al. Cortical hubs revealed by intrinsic functional connectivity: mapping, assessment of stability, and relation to Alzheimer's disease. *J Neurosci*. 2009;29:1860–1873.
8. Drzezga A, Becker JA, Van Dijk KR, et al. Neuronal dysfunction and disconnection of cortical hubs in non-demented subjects with elevated amyloid burden. *Brain*. 2011;134:1635–1646.
9. Bassett DS, Bullmore E, Verchinski BA, Mattay VS, Weinberger DR, Meyer-Lindenberg A. Hierarchical organization of human cortical networks in health and schizophrenia. *J Neurosci*. 2008;28:9239–9248.
10. Li X, Xia S, Bertisch HC, Branch CA, Delisi LE. Unique topology of language processing brain network: a systems-level biomarker of schizophrenia. *Schizophr Res*. 2012;141:128–136.
11. Chen Y, Bidwell LC, Holzman PS. Visual motion integration in schizophrenia patients, their first-degree relatives, and patients with bipolar disorder. *Schizophr Res*. 2005;74:271–281.
12. Hamm JP, Ethridge LE, Shapiro JR, et al. Spatiotemporal and frequency domain analysis of auditory paired stimuli processing in schizophrenia and bipolar disorder with psychosis. *Psychophysiology*. 2012;49:522–530.
13. Curtis VA, Dixon TA, Morris RG, et al. Differential frontal activation in schizophrenia and bipolar illness during verbal fluency. *J Affect Disord*. 2001;66:111–121.
14. Ongür D, Lundy M, Greenhouse I, et al. Default mode network abnormalities in bipolar disorder and schizophrenia. *Psychiatry Res*. 2010;183:59–68.
15. Ellison-Wright I, Bullmore E. Anatomy of bipolar disorder and schizophrenia: a meta-analysis. *Schizophr Res*. 2010;117:1–12.
16. Kraepelin E. *Dementia praecox and paraphrenia*. 8th ed. Edinburgh, UK: Livingstone; 1919.
17. Leckman JF, Sholomskas D, Thompson WD, Belanger A, Weissman MM. Best estimate of lifetime psychiatric diagnosis: a methodological study. *Arch Gen Psychiatry*. 1982;39:879–883.
18. Liddle PF, Ngan ET, Duffield G, Kho K, Warren AJ. Signs and Symptoms of Psychotic Illness (SSPI): a rating scale. *Br J Psychiatry*. 2002;180:45–50.
19. Ammons RB, Ammons CH. The Quick Test (QT): provisional manual. *Psychol Rep*. 1962;11:111–161.
20. WHO Collaborating Centre for Drug Statistics and Methodology. *Guidelines for ATC Classification and DDD Assignment*. Oslo, Norway: WHO Collaborating Centre for Drug Statistics and Methodology; 2003.
21. Rose D, Pevalin DJ. *A Researcher's Guide to the National Statistics Socio-economic Classification*. London: Sage Publications; 2003.
22. Gowland PA, Bowtell R. Theoretical optimization of multi-echo fMRI data acquisition. *Phys Med Biol*. 2007;52:1801–1813.
23. Chao-Gan Y, Yu-Feng Z. DPARSF: A MATLAB Toolbox for "Pipeline" Data Analysis of Resting-State fMRI. *Front Syst Neurosci*. 2010;4:13.
24. Dale AM, Fischl B, Sereno MI. Cortical surface-based analysis. I. Segmentation and surface reconstruction. *Neuroimage*. 1999;9:179–194.
25. Schaer M, Cuadra MB, Tamarit L, Lazeyras F, Eliez S, Thiran JP. A surface-based approach to quantify local cortical gyrification. *IEEE Trans Med Imaging*. 2008;27:161–170.
26. Zou KH, Warfield SK, Bharatha A, et al. Statistical validation of image segmentation quality based on a spatial overlap index. *Acad Radiol*. 2004;11:178–189.
27. Duncan KJ, Pattamadilok C, Knierim I, Devlin JT. Consistency and variability in functional localisers. *Neuroimage*. 2009;46:1018–1026.
28. Palaniyappan L, Liddle PF. Does the salience network play a cardinal role in psychosis? An emerging hypothesis of insular dysfunction. *J Psychiatry Neurosci*. 2012;37:17–27.
29. Meyer-Lindenberg AS, Olsen RK, Kohn PD, et al. Regionally specific disturbance of dorsolateral prefrontal-hippocampal functional connectivity in schizophrenia. *Arch Gen Psychiatry*. 2005;62:379–386.
30. Collin G, Hulshoff Pol HE, Haijma SV, et al. Impaired Cerebellar Functional Connectivity in Schizophrenia Patients and Their Healthy Siblings. *Front Psychiatry*. 2011;2. http://www.ncbi.nlm.nih.gov/pmc/articles/PMC3240868/. Accessed November 19, 2012.
31. Palaniyappan L, Liddle PF. Aberrant cortical gyrification in schizophrenia: a surface-based morphometry study. *J Psychiatry Neurosci*. 2012;37:399–406.
32. Palaniyappan L, Mallikarjun P, Joseph V, White TP, Liddle PF. Folding of the prefrontal cortex in schizophrenia: regional differences in gyrification. *Biol Psychiatry*. 2011;69:974–979.
33. Schmitt A, Schulenberg W, Bernstein HG, et al. Reduction of gyrification index in the cerebellar vermis in schizophrenia: a post-mortem study. *World J Biol Psychiatry*. 2011;12(Suppl 1):99–103.
34. Kumar CT, Christodoulou T, Vyas NS, et al.. Deficits in visual sustained attention differentiate genetic liability and disease expression for schizophrenia from Bipolar Disorder. *Schizophr Res*. 2010;124:152–160.
35. Braddick O, Atkinson J, Wattam-Bell J. Normal and anomalous development of visual motion processing: motion coherence and 'dorsal-stream vulnerability'. *Neuropsychologia*. 2003;41:1769–1784.
36. Sui J, Pearlson G, Caprihan A, et al. Discriminating schizophrenia and bipolar disorder by fusing fMRI and DTI in a multimodal CCA+ joint ICA model. *Neuroimage*. 2011;57:839–855.

37. Delvecchio G, Sugranyes G, Frangou S. Evidence of diagnostic specificity in the neural correlates of facial affect processing in bipolar disorder and schizophrenia: a meta-analysis of functional imaging studies. *Psychol Med*. 2013;43:553–569.
38. Calhoun VD, Sui J, Kiehl K, Turner J, Allen E, Pearlson G. Exploring the psychosis functional connectome: aberrant intrinsic networks in schizophrenia and bipolar disorder. *Front Psychiatry*. 2011;2:75.
39. Hafeman DM, Chang KD, Garrett AS, Sanders EM, Phillips ML. Effects of medication on neuroimaging findings in bipolar disorder: an updated review. *Bipolar Disord*. 2012;14:375–410.
40. Lui S, Li T, Deng W, et al. Short-term effects of antipsychotic treatment on cerebral function in drug-naive first-episode schizophrenia revealed by "resting state" functional magnetic resonance imaging. *Arch Gen Psychiatry*. 2010;67:783–792.
41. Fusar-Poli P, Howes O, Bechdolf A, Borgwardt S. Mapping vulnerability to bipolar disorder: a systematic review and meta-analysis of neuroimaging studies. *J Psychiatry Neurosci*. 2012;37:170–184.
42. Smieskova R, Fusar-Poli P, Allen P, et al. Neuroimaging predictors of transition to psychosis–a systematic review and meta-analysis. *Neurosci Biobehav Rev*. 2010;34:1207–1222.